Original

Design and implementation of an alternative measurement system for MOSFET-Like sensors characterization

Luighi Viton-Zorrilla[*], Jinmi Lezama, Rubén Acosta, Milton Ríos-Julcapoma

Instituto Nacional de Investigación y Capacitación de Telecomunicaciones (INICTEL-UNI)
Universidad Nacional de Ingeniería, Perú

Abstract: This paper describes the design and implementation of an alternative system to measure electrical parameters (voltage and current) in order to characterize MOSFET-Like sensors. To design a signal conditioning circuit is necessary to understand the sensor behavior, therefore knowing its characteristics is essential. As sensor manufacturers do not usually provide the whole technical information about them, a measurement system is proposed to obtain those sensor characteristics with the aim of modeling the sensor device. This system is based on a MCU which generates voltages and measures currents via an external transimpedance amplifier, and it is supported by a software platform developed upon python based open source tools. Such combination offers a low cost system to stimulate and capture sensor responses which could be processed later to extract the characteristic parameters. The system was tested principally with an Ion Sensitive Field Effect Transistor (ISFET) and results show the V_{DS}-I_{DS} and V_{GS} curves obtained with it.

Keywords: measurement system, sensor characterization, MCU, ISFET

1. INTRODUCTION

Signal conditioning is an essential topic in the process of designing readout circuits, where the most important information of the sensors are the physical and electrical characteristics. Despite the fact that essential parameters are provided by sensors datasheet, there are some manufacturers which do not offer some or the whole technical information. Therefore, it is necessary to find the optimal values which describes them appropriately and adjust the electrical model to the real device responses. Also, it is important for testing purposes, to evaluate its behavior in the intended environment.

[*] Corresponding author.

E-mail address: luighi.viton.z@uni.pe (Luighi Viton-Zorrilla).

Electrical parameters are the most common measurements and among them, voltages and currents are the simplest to acquire. In case of semiconductor based devices, in special MOSFETs and derived ones such as ISFETs (Bergveld, 1981), they rely on those magnitudes to extract their fundamental parameters (Haddara, 1995).

To obtain these values it is nevertheless required a specialized equipment (Keithley, A Tektronix Company, 2016b). Taking the ISFET as an example, at least 3 SMUs and a parameter analyzer are needed (Martins & Rangel, 2012; Yusof et al., 2013). Although SMUs provide a plenty of features to an accurate measurement (Keysight, 2016), in some cases, only a few of them are required to obtain the desired response.

For many applications such as device characterizations, SMUs combines capabilities from a precision power supply and a digital multimeter, incorporating a great speed and

resolution, four-quadrant operation and sweeps (Cejer, Tucker, & Weng, 2013). All of them are employed in a wide range of applications, for instance, nanomaterials, energy efficiency, material characterization, semiconductor structures and so on (Keithley, A Tektronix Company, 2016a, 2016c).

However, there are some which do not demand exhaustive precision, high voltages or currents; moreover, considering that its cost makes this solution unaffordable when it is part of small projects. For example, in low power devices such as ISFETs, whose currents are up to $80\mu A$ and voltages do not exceed 2.0V. Additionally, their resolution is not a critical issue when performing qualitative measurements.

ISFET characterizations are analyzed from the I_D vs V_D and I_D vs V_G curves. Previous work shows some techniques to acquire this data. For example, (Rani, Syono, & Ramli, 2008) got these curves using Agilent semiconductor device analyzer, (Mayorga, Aldana, & Rodriguez, 1997) have presented a system based in a microcontroller to obtain them, while (Villalpando, Miranda, Martinez, & Martinez, 2012) got the curves using a HACH Measurement instrument. All of the cited authors have presented different systems to obtain the current and voltage curves, and these results show the performance of the ISFET device for different conditions.

Acquiring data is usually not enough as storing it in some way is also important. For these approach it is demanding a PC communication to record and visualize such information. Solutions found employ LabVIEW and MatLab (Catelani & Ciani, 2013; Midili, 2012) to perform this function. However, being a proprietary software, limits its use to computers with an active license only.

Hence, the aims of this work are to provide a low-cost system which could acquire the current-voltage characteristic from MOSFET based sensors, transfers this data controlled via a PC and provide a platform to add different scripts for analysis without restrictions of licenses.

2. SYSTEM DESIGN AND DEVELOPMENT

The proposed system involves an electronic and computational approach to obtain the characteristic of the sensor based on MOSFET. This system is composed by a voltage generator to stimulate the sensor and a current measure to capture its response (Figure 1).
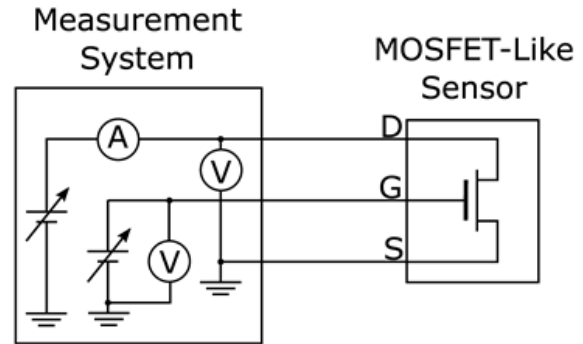

Fig. 1. Conceptual measurement system.

It is constituted by three main components: the hardware deployment, essentially conformed by a MCU, the firmware, which manages the hardware in first instance and the software environment, which interacts with the user.

Open source platform of hardware and software was used to develop the system, hence it is designed to perform two modes of operation: automatic and manual. The manual mode allows the user to change the voltage source value either to the next or previous step, while the automatic mode changes this value automatically, generating an escalator waveform.

In comparison with existing solutions, this design allows to choose different voltage source varying its waveform (ramp, escalator, constant and others). Moreover, it allows to add scripts to analyze and process data (FFT, filters, arithmetic operation).

An ISFET sensor was used to test the system and experiments were conducted to obtain current and voltages measures for different pH values. The results provides the curves $V_{DS} - I_{DS}$ and $V_{GS} - I_{DS}$ to extract the sensor characteristics.

3. HARDWARE DESCRIPTION

As the system is thought to be used as a characterization instrument, is precise to provide it the ability to interact with external signals. This means, it must include some components such as ADCs and DACs to generate and acquire analogue stimulus. Additionally, as current is an important magnitude to be measured, a transducer is attached to convert them to voltages.

The control of each component is performed remotely as well as the visualization, so it includes an UART module to communicate with the CPU. In addition to this,

an external interruption is provided to control some basic functions manually.

As it is shown in Figure 2, there is a microcontroller which is responsible to perform the required functionality and an external board to measure the sensor current response.

The MCU owns two DACs, two ADCs and two timers, whose control is passed through the microprocessor to the external interruption and the UART module. Both ADCs are connected to the timer TIM8 which triggers and regulates the time between two successive conversions. The another timer, TIM6, is connected to the DAC in order to trigger it and establish the step period in the escalator waveform.

The auxiliary board is committed to perform analogue features as it is responsible to transform current into voltage levels. It is essentially comprised by a transimpedance amplifier (TIA) which receives the current from the sensor and, via a resistance in feedback, converts this current into a voltage signal. As the current is positive the voltage output is higher than the voltage in the reference terminal attached to the DAC2 output.

4. FIRMWARE DESCRIPTION

As soon as the module is power on, all the components required are initialized and started in the MCU. The process starts with the main clock activation and the routine of initialization. Afterwards, the peripherals (DACs, ADCs, Timers and GPIOs) and communication modules (UART) are initialized.

The Figure 3 shows the main process executed in the MCU. As soon as the components are initialized, the ADC and TIM8 start their activity enabling the acquisition process. Then, an infinite loop starts, where it is performed the MCU behavior change as well as the communication via UART, both for transmission and reception purposes. There are four flags used to control the process. Those are: *ubKeyPressed*, *manual*, *UARTReady* and *ConvCompleted*.

- The *ubKeyPressed* flag which indicates an external interruption and used to change the operation mode.
- The *manual* flag used to store the operation mode, manual or automatic, depending on its state.
- The *UARTReady*, which sets the DAC value, based in the instruction obtained from the UART, either to the next or previous one, depending if the *manual* flag is set. Then, it starts again the receiving process and disable the flag.
- The *ConvCompleted*, which transmits the transmission buffer via UART with information about ADC, DAC, TIM and Control.

The flags mentioned before are disabled by default, and they are activated in the interruption processes. There are three considered in this firmware: the external interruption, the ADC conversion completed interruption and the UART reception completed interruption.

- *External interruption.* This interruption allows the user to switch between the manual and automatic operation mode. It is done through toggling the *ubKeyPressed* flag.
- *ADC conversion completed.* This interruption extract data from ADCs and store in the
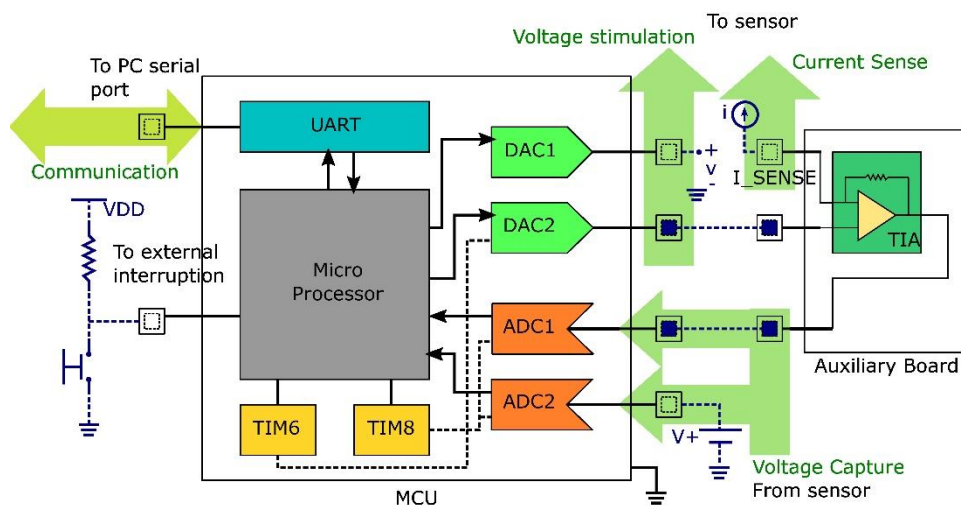

Fig. 2. Hardware component description.

transmission buffer. Then when it reaches a certain number of times (10 in this case), the process appends the DAC value, TIM register and control flag. Finally, it sets the *ConvCompleted* flag. This is shown in Figure 4.

- *UART reception completed.* Based on the value received, it compares with strings to determine the functions to be performed. In this case, the strings used were: "nn" for the next instruction, "pp" for the previous instruction, "aa" for the automatic instruction and "mm" for the manual instruction. Manual or automatic instructions activate *ubKeyPressed* and *manual* flags, simulating the external interruption and setting the corresponding mode. Next or previous instructions check the data to prevent overflow, and then sets the DAC to its corresponding value. This is depicted in Figure 5.
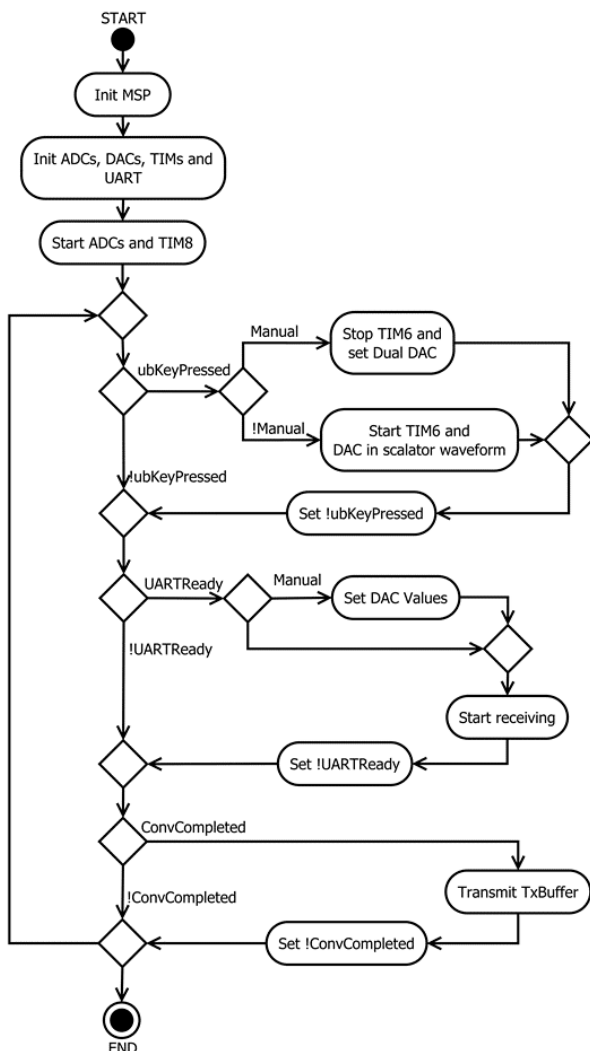

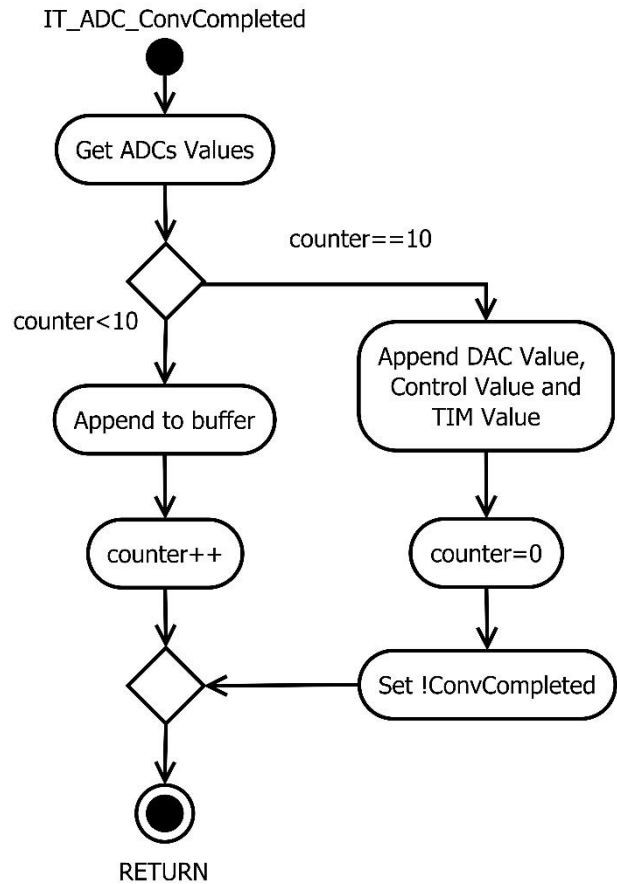Fig. 3. Main process firmware.

Fig. 4. Interruption process when ADC finish conversion.

Another important topic to highlight is the data sent by the UART. In this case, it has the ASCII format so it is easier to debug in any serial terminal. On the other hand, besides that UART operations demand larger CPU times, it is convenient to send more data in each message rather than only few bytes which could imply more information losses. The approach considered here is storing the data acquired in a temporary buffer while UART is being used, until it is sent in the next transmission process.

The data frame has the following structure:

$$\underbrace{ADC1, ADC2: ADC1, ADC2: \ldots : ADC1, ADC2}_{10\ times}\#DAC\#TIM\#Ctrl\backslash n \qquad (1)$$

The "ADC1" and "ADC2" correspond to the conversions obtained from the ADC1 and ADC2 in the module. Then "DAC" represents the value established in the DAC2, the "TIM" is the timer register and "Ctrl" corresponds to the manual flag used as a feedback for the software environment.
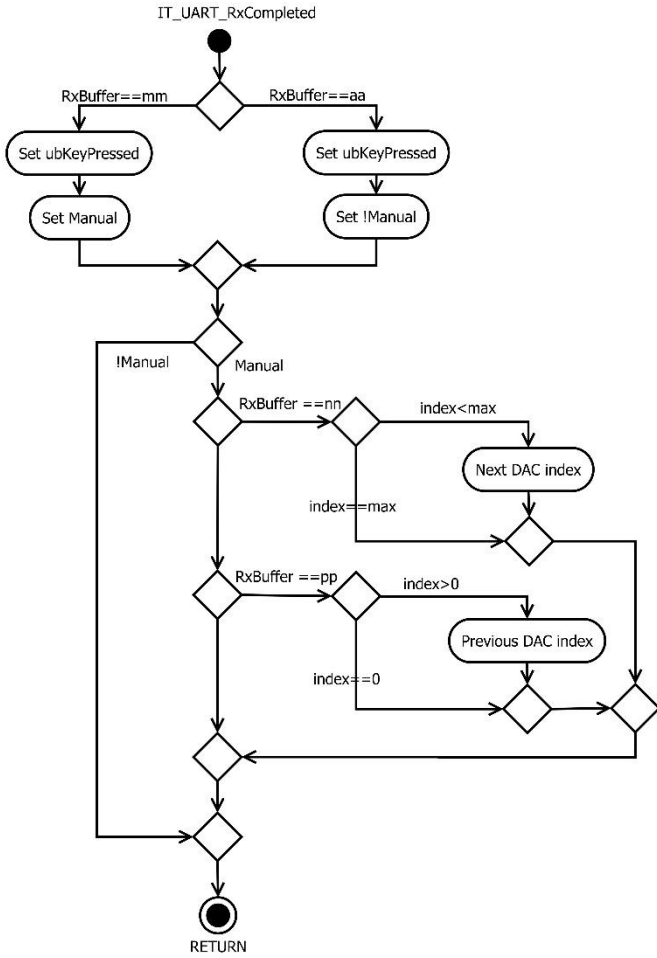
Fig. 5. Interruption process when
UART receives message.

5. SOFTWARE DESCRIPTION

The software environment consist of two main modules which are the *SerialModule* and the GUI. The first one runs in background and performs the operation to communicate with the hardware while the second one, constitutes the foreground and serve as platform to interact with users. Figure 6 portraits these two components.

The GUI component is inherited from *MeasureMainContents* which is inherited also from *MainWindow*. The last one is used to provide the external tools (menubar, statusbar, toolbar, contextmenu), general for every application window while MeasureMainContents places the components required to communicate with serial module. These components are:

- *ConnectionModule.* Provides functions to enter the serial parameters. This is presented to users as a dialogue via *SettingsDialog*.
- *ControlDACModule.* Provides buttons to switch between operations modes. Also, it includes two more buttons: Next and Previous to change values in the DAC when is in manual mode, and shows the timer counter as a progress bar when is in automatic mode.
- *ControlButtons.* Allows the user to start acquiring data from serial module and interacts with the hardware. For these functions, the module has two buttons, one to start the process and another to finish it.
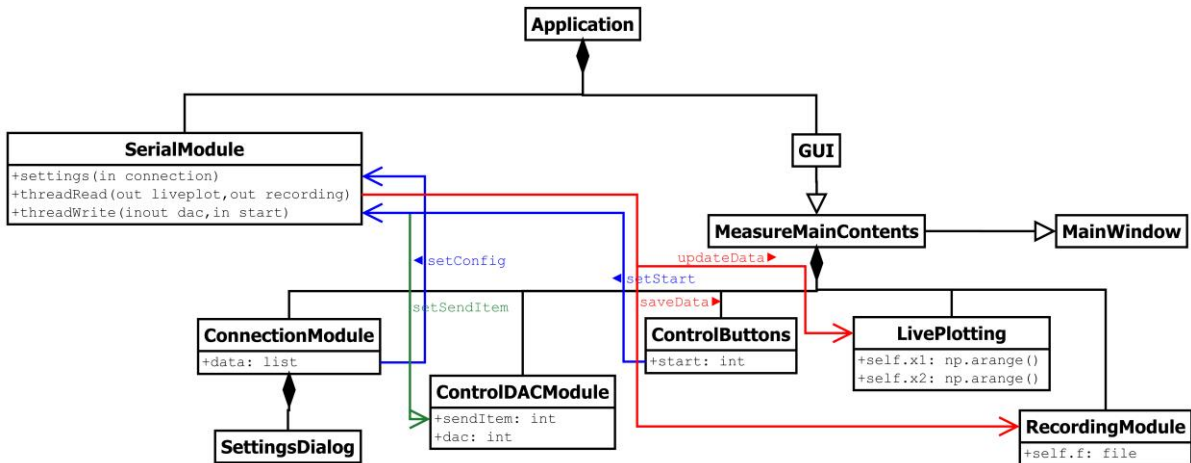

Fig. 6. Software structure.

- *LivePlotting.* Render data acquired from serial. It also has a cursor to show current values at a certain position.
- *RecordingModule.* Allows the user to record data acquired from serial and saves that in a plain text file.

On the other hand, the *SerialModule* is able to communicate with the hardware, providing some functions to receive information from the GUI and set variables to this one. The principal functions are:

- *Settings.* Which receives information from the *ConnectionModule* and configures the parameters of the serial port.
- *ThreadRead.* Which implements an independent thread to acquire data from the serial port. It sets internal variables of *LivePlotting* to render the waveforms and stores data acquired in a temporary file while the recording module is active. In addition to this, it sets the information regarding the current value in the DAC and the timer counter.
- *ThreadWrite.* Also implements an independent thread and sends commands to the hardware from the GUI. This receives information from the *ControlDACModule*, to send the manual ("mm") or automatic ("aa") mode controls, or the previous ("pp") or next ("nn") instruction controls.

The sequence of operation in the software is depicted in Figure 7. Here, when the user open the program it immediately creates the interface modules and the serial module.

Then, through the *ConnectionModule*, the user could open a Dialogue to set the serial port parameters and these values are returned to the main module and set in the serial one. The interaction process between the software and hardware starts once the user press the start button. This action creates two threads with the functions provided for the serial module to read and write in the serial port. Hence, the read and write processes are enabled.

The read process consists in continuous requests made from the thread to the serial port. This returns the read value and based on the information provided, updates variables in *LivePlotting* and *ControlDACModule*. The writing process is a result of the user interaction, which changes a value in the *ControlDACModule*. Then, this sends the message to the thread which, at the same time, writes to the serial port.

Finally, once stop button is pressed, the stop routine is triggered, destroying the threads created before and stopping the visualization, data acquisition and interaction process.
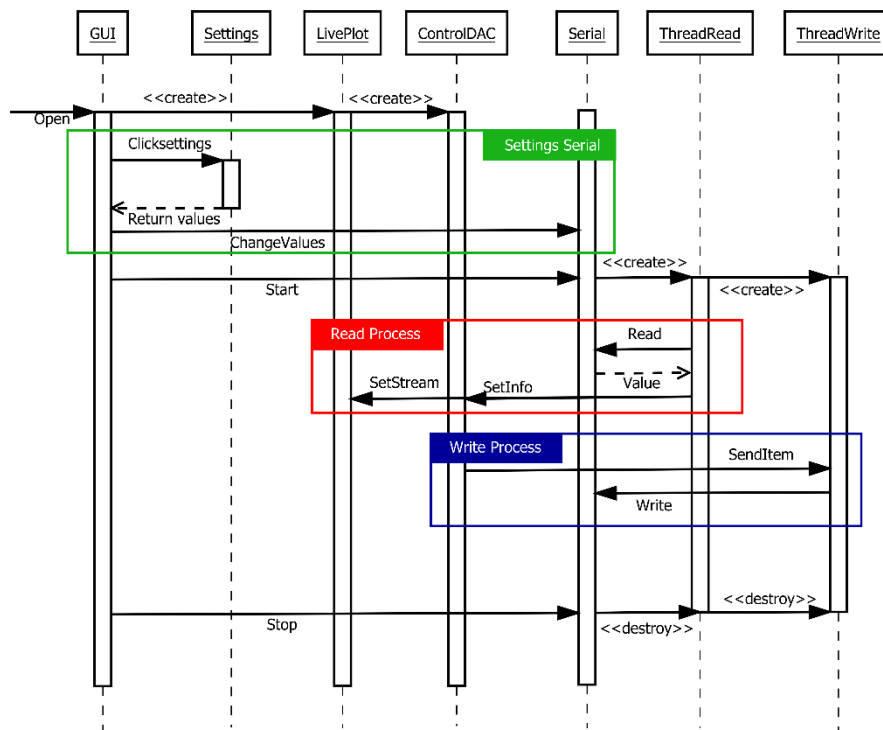

Fig. 7. Software sequence.

Data acquired from the software need to be processed later to obtain the characteristic curves. The processing steps are depicted in Figure 8. It comprises a series of filters to remove the noise introduced by external sources as well as the quantization process in ADCs. Those steps are:

Median filter. Which removes impulsive noise in the signal presented as discrete discontinuities with no correspondence with the curve tendency.

Moving average filter. Used to remove irregularities due to different noise sources including those occasioned by quantization process in ADCs.

Mask. Used to classify each segment in the signal which represents a particular point in the current-voltage curve, result of the characterization process.

Mean. Used to obtain the representative value for each segment classified by the mask. The set of values obtained constitutes the full current-voltage curve.

The process mentioned before is applied to each curve obtained from the measurement system so a set of curves is obtained after the processing task corresponding to the curve family for a particular test.

6. IMPLEMENTATION

The hardware component is formed by the microcontroller STM32F407VGT6 (STMicroelectronics, 2016c, 2016b) which is part of the STM32 F4 Discovery board (STMicroelectronics, 2016d).

The toolchain used to program the main MCU was System Workbench for STM32 (AC6, 2016), from AC6. Additionally, the HAL drivers (STMicroelectronics, 2016e) and examples (STMicroelectronics, 2016a) provided in

Table 1. Microcontrollers characteristics.

Name	Characteristics
CPU	ARM 32-bit Cortex-M4
FREQUENCY	168 MHz
ADCs	3x12-bit, 2.4 MSPS or 7.2 MSPS
DACs	2x12-bit, 2.4 MSPS
COMMUNICATIONS	2xUARTs, 3xSPI, 3xI2C, 2xCAN, SDIO

STM32CubeF4 (STMicroelectronics, 2015, 2016f) were used to manage the MCU configuration. Table 1 shows STM32 microcontroller characteristics.

An auxiliary board is designed to convert the current, produced by interaction between the test solution and ISFET, into a voltage signal. This circuit is based on a TIA, which is comprised by a LM324 operational amplifier and a resistance in feedback (R_f). Where R_f value is selected in function of the ISFET characteristics such as the maximum current tolerance of $80\mu A$ and the maximum voltage of 2.0V. Considering a battery operated system with 3.6V, the TIA voltage output must be under this value. In the worst case, this voltage is $2.0 + 80\mu \times R_f$, then R_f value is chosen approximately equal to $20k\Omega$.

The software implementation was made in python via the Python(x,y) distribution (Raybaut & Davar, 2015). It includes a range of libraries to do numerical calculations such as numpy (NumPy developers, 2016). The interface was implemented using PyQt libraries (Riverbank, 2016). In addition to this, the pyqtgraph module (Campagnola, 2016) was installed to implement the monitoring widget.
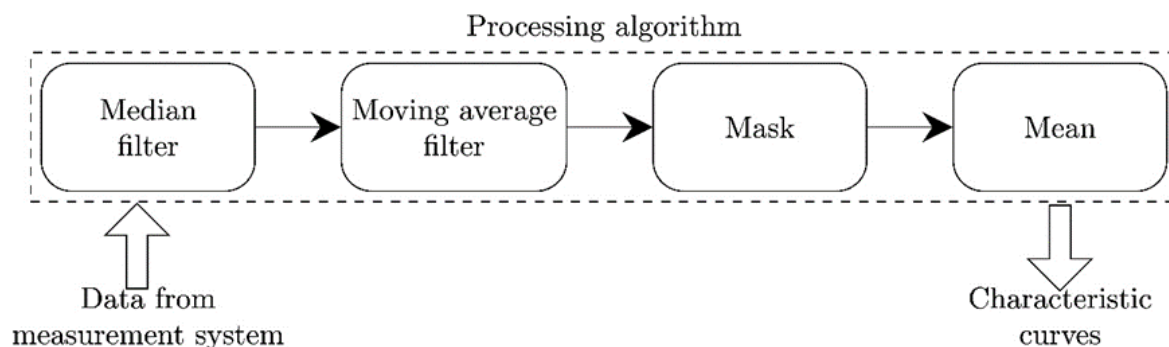

Fig. 8. Processing algorithm to obtain characteristic curves.

7. TESTBENCH CIRCUIT

In order to test the system functionality it was connected to probe an ISFET sensor (Bergveld, 1981). This device has the particularity to respond to pH changes with variations in its drain current. However, to characterize this sensor is required to obtain its characteristic curves, from which extract its parameters. The ISFET current equation is very similar to the MOSFET as it is presented in (2).

$$I_D = K\frac{W}{L}\left(V_{GS} - V_{TH_{ISFET}} - \frac{V_{DS}}{2}\right)V_{DS} \qquad (2)$$

Where K is the transconductance coefficient characteristic of the ISFET material, W is the channel width, L is the channel length and $V_{TH_{ISFET}}$ is the threshold voltage which has a dependence with respect to the pH of the test solution.

As the ISFET has a similar behavior as the MOSFET, the circuit to test this device not differ too much from the

last one (Liou, Ortiz-Conde, & Garcia-Sanchez, 1998; Martins & Rangel, 2012). In fact, the employed circuit consists in two sources which provide the V_{GS} and V_{DS} voltages. These sources are both DACs in the measurement system. Additionally, one ADC is connected to the TIA output from the auxiliary board and a second ADC to the V_D terminal. This scheme is shown in Figure 9 (a). The device used in this experiment was manufactured by WINSENSE which has a maximum current tolerance of $80\mu A$, while V_{DS} voltage should not exceed 2.0V (WINSENSE, 2016).

8. RESULTS

Once the system testbench was appropriately connected, an automatic measurement process was started to obtain the values of the gate-source voltage (V_{DS}), directly from the ADC attached to the drain terminal, and the drain current (I_D) from the difference between the first one and the ADC connected to the TIA output. The voltage range provided by the DAC in V_{DS} (which performs the escalator waveform) is between 40mV to 1.93V accomplishing the device tolerance.

The implementation with the mentioned conditions is shown in Figure 9 (b), where all devices are put together to perform the test and to extract the required data. The software GUI developed in python is presented in Figure 10, pointing out each of its components.

Data obtained from the measurement system is depicted in the Figure 11. An automatic test is executed where an increase of voltage is performed each 10 seconds. The generated waveform is an escalator where the voltage from TIA is above the voltage reference and the difference between them is proportional to the current in the sensor. As the total of steps per curve is 42 in a complete test, the time per test is approximately 420s=7min.

In the Figure 12 and Figure 13, results of two group of measurements are depicted after their processing. Those were taken in different times and processed later employing the algorithm presented in Figure 8 to obtain the voltage and current values required to characterize the device. The voltages used to stimulate the sensor were 750mV and 850mV at V_{GS}, placed in a 7.0 pH buffer both.

As it is shown, there are some differences among those measurements, regarding the variation of temperature and hysteresis presented in the ISFET.
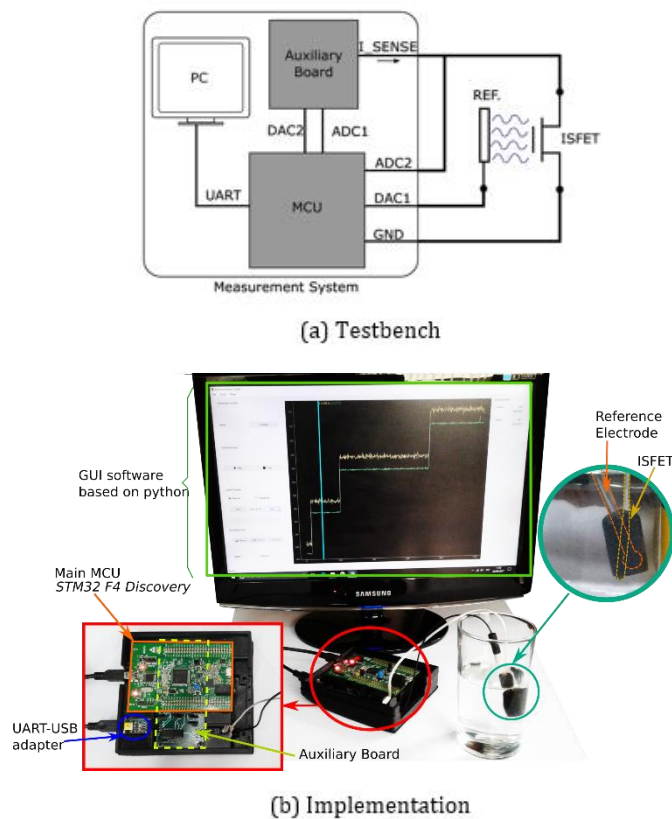

(a) Testbench

(b) Implementation

Fig. 9. System implementation.

Figure 14 shows the curve I_{DS} vs V_{DS} for different values of V_{GS} and a pH=7. These results show the ISFET sensor characteristics for different reference voltages V_{GS}.

Figure 15 shows the variation of I_{DS} for different V_{DS}. The results of these curves allow to calculate the threshold voltage V_{TH} and saturation current I_S from which it is possible to extract the transconductance coefficient $K = u_{eff}C_{eff}$ necessary to introduce in the device model presented in (2) (Martinoia & Massobrio, 2000; Tomaszewski, 2007).
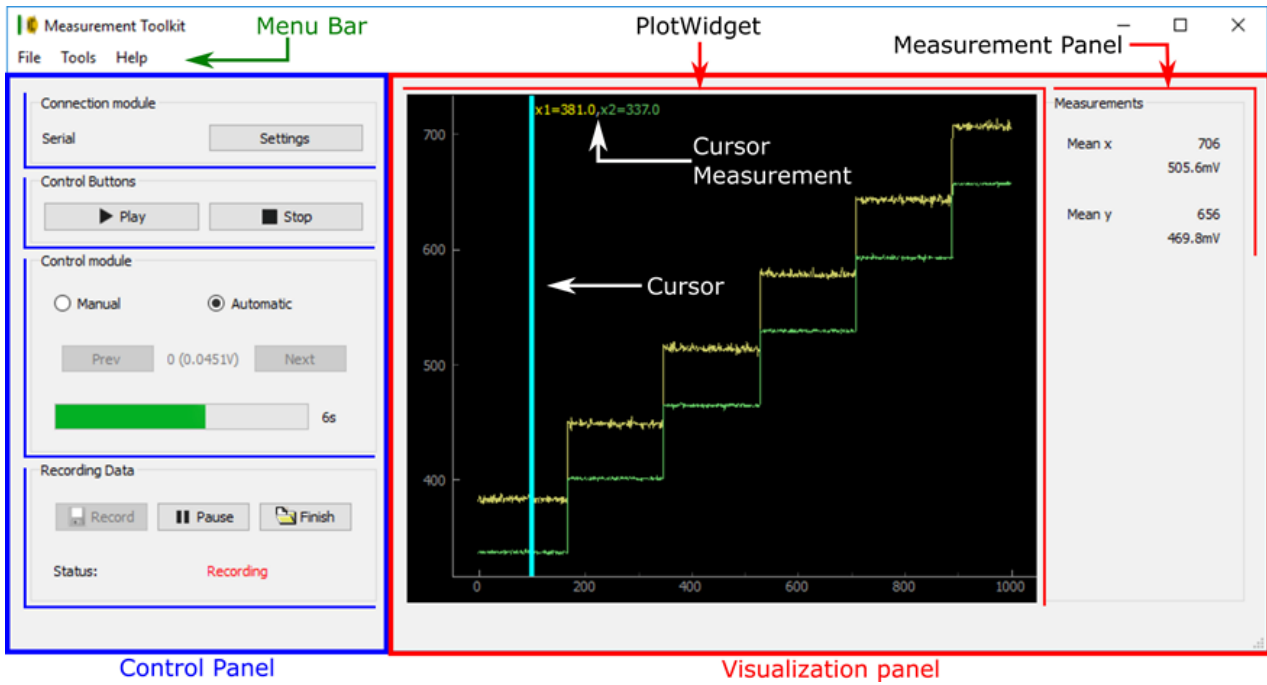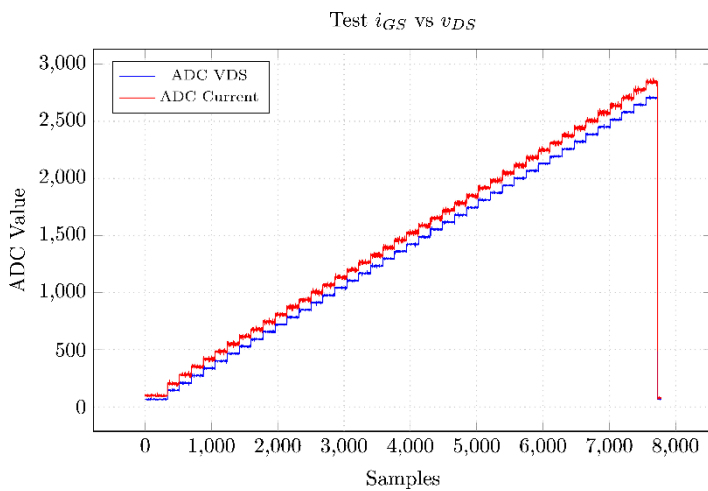

Fig. 10. GUI implemented in python.

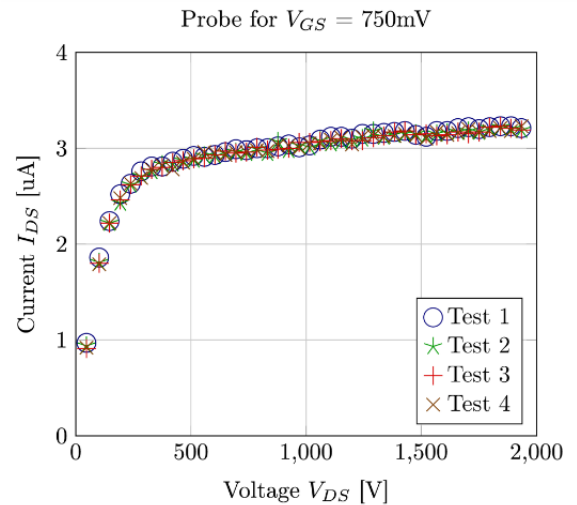Fig. 11. Data acquired for I_{DS} vs. V_{DS} with V_{GS}=905mA.

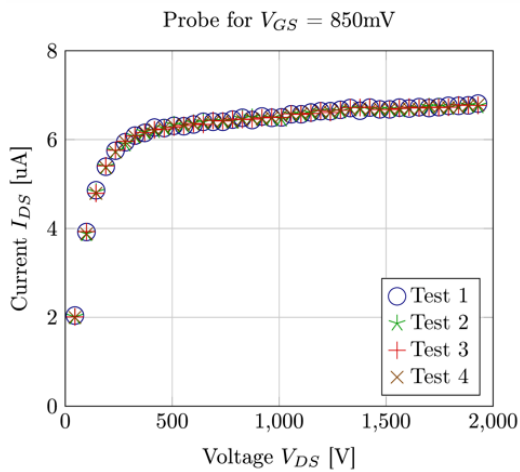Fig. 12. Variation V_{DS} vs I_{DS} curve at pH7, V_{GS}= 750Mv.

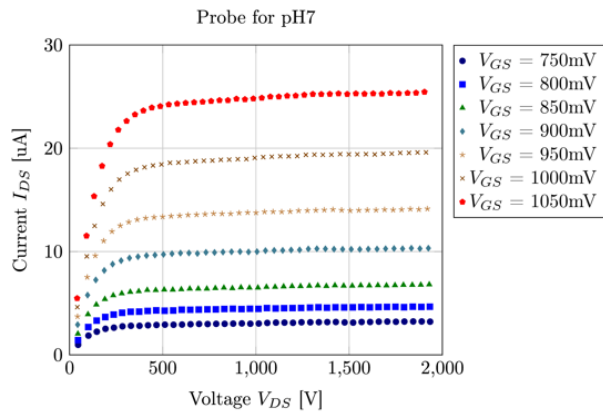Fig. 13. Variation V~DS~ vs I~DS~ curve at pH7,
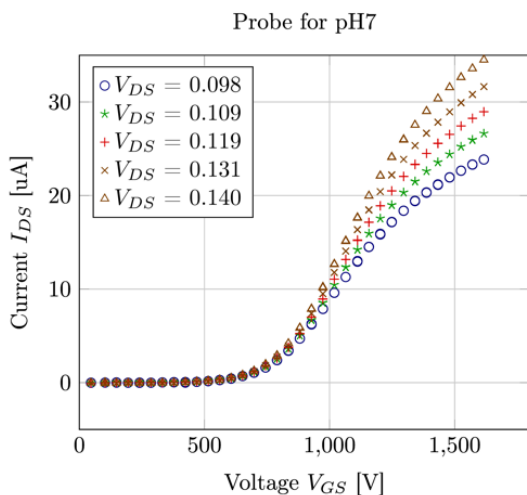V~GS~= 850mV.

Fig. 14. V~DS~ vs I~DS~ curve at pH7.

Fig. 15. V~GS~ vs I~DS~ curve at pH7.

9. CONCLUSION

To obtain electrical parameters of sensors is necessary to use SMUs and a parameter analyzer, which can represent a costly solution. In this paper, open source tools are employed to develop a low-cost measurement system based on embedded devices in order to characterize sensors and fit their electrical model to real devices. Thanks to the flexibility of being programmable and its ability to manage analogue components, the system provides a sufficient tool toanalyze sensors behavior and extract from measurements the main parameters which govern their responses.

The system was tested with an ISFET device and the V-I curves obtained show a great agreement with the theoretical parametric curves. Despite of noise introduced by connections, it is not significant as it could be removed easily with some processing tasks. However, it is only useful if currents are higher than $0.02\mu A$ as it is the precision for the given system. On the other hand, this is limited to DACs current constraints, which are up to $280\mu A$ (STMicroelectronics, 2016c).

Future works will be oriented to extend its capability to other sensors incorporating more electrical parameters such as capacitance or resistance. Additionally, the feature to restrict current levels will be implemented.

ACKNOWLEDGMENTS

CONFLICT OF INTEREST

The authors have no conflicts of interest to declare.

REFERENCES

AC6. (2016). System workbench for stm32. Retrieved from http://www.openstm32.org/System+Workbench+for+ST M32

Bergveld, P. (1981). The operation of an ISFET as an electronic device. *Sensors and Actuators*, *1*(C), 17–29. doi: 10.1016/0250-6874(81)80004-2

Campagnola, L. (2016). PyQtGraph scientific graphics and gui library for python. Retrieved from http://www.pyqtgraph.org/

Catelani, M., & Ciani, L. (2013). Design And Implementation Of An Automatic Measurement System For The Characterization Of Power MOSFETs. In *19th imeko tc 4 symposium and 17th iwadc workshop*. Retrieved from https://pdfs.semanticscholar.org/8134/9767ccf8220a445a16d88380c06947ee8e60.pdf

Cejer, M. A., Tucker, J. L., & Weng, L. (2013). *Choosing the optimal source measurement unit instrument for your test and measurement application*. Keithley Instruments, Inc. Retrieved from http://www.tek.com/sites/tek.com/files/media/document/resources/HowToCHooseSMU.pdf

Haddara, H. (1995). *Characterization Methods for Submicron MOSFETs*. Springer, Boston, MA. doi: 10.1007/978-1-4613-1355-7

Keithley, A Tektronix Company. (2016a). *2450 sourcemeter smu instrument datasheet*. Retrieved from http://www.tek.com/sites/tek.com/files/media/media/resources/1KW-60904-0_2450_DataSheet_0.pdf

Keithley, A Tektronix Company. (2016b). *Simplifying FET Testing with 2600B System SourceMeter® SMU Instruments -- Application Note*. Retrieved from https://www.tek.com/document/application-note/simplifying-fet-testing-series-2600b-system-sourcemeter-smu-instruments

Keithley, A Tektronix Company. (2016c). *SourceMeterSMU instrument 1000 watts, 10 amps pulse, 7 amps dc*. Retrieved from http://www.tek.com/sites/tek.com/files/media/media/resources/2461-DataSheet.pdf

Keysight. (2016). *Keysight Technologies B2900A Series Precision Source/Measure Unit*. Retrieved from http://literature.cdn.keysight.com/litweb/pdf/5990-7009EN.pdf

Liou, J. J., Ortiz-Conde, A., & Garcia-Sanchez, F. (1998). *Analysis and Design of MOSFETs*. Boston, MA: Springer US. doi: 10.1007/978-1-4615-5415-8

Martinoia, S., & Massobrio, G. (2000). Behavioral macromodel of the ISFET in SPICE. *Sensors and Actuators, B: Chemical*, *62*(3), 182–189. doi: 10.1016/S0925-4005(99)00377-9

Martins, R., & Rangel, F. (2012). An Analog Front-End for an ISFET-Based Sensor Using Off-The-Shelf Components, *1*. Retrieved from http://lrf.ufsc.br/files/2012/07/48_Final_Manuscript.pdf

Mayorga, O., Aldana, G., & Rodriguez, H. (1997). Microcontroller-based system for multiple isfet characterization using a single reference electrode. In *Engineering in medicine and biology society, 1997.*

Proceedings of the 19th annual international conference of the IEEE. 6, 2361–2364. doi: 10.1109/IEMBS.1997.756791

Midili, V. (2012). *Realization of a capacitance-voltage measurement system for semiconductor characterization* (Master's thesis). Aalto University. Retrieved from https://pdfs.semanticscholar.org/1639/980255ba8203de93c0669737d799f984c32e.pdf

NumPy developers. (2016). NumPy. Retrieved from http://www.numpy.org/

Rani, R. A., Syono, M. I., & Ramli, A. S. (2008). Characterizations of single gate and multi-finger gate of isfet for pH sensor applications. In *2008 9th international conference on solid-state and integrated-circuit technology* (pp. 2577–2580). doi: 10.1109/ICSICT.2008.4735099

Raybaut, P., & Davar, G. (2015). Python(x,y) - the scientific python distribution. Retrieved from http://python-xy.github.io/

Riverbank. (2016). PyQt4 reference guide. Retrieved from http://pyqt.sourceforge.net/Docs/PyQt4/

STMicroelectronics. (2015). *STM32CubeF4*. Retrieved from http://www.st.com/content/ccc/resource/technical/document/data_brief/5b/fc/ce/cb/7b/71/4a/1c/DM00103572.pdf/files/DM00103572.pdf/jcr:content/translations/en.DM00103572.pdf

STMicroelectronics. (2016a). *AN4739 application note: STM32Cube firmware examples for stm32f4 series*. Retrieved from http://www.st.com/content/ccc/resource/technical/document/application_note/ca/34/db/d3/71/50/44/9b/DM00213525.pdf/files/DM00213525.pdf/jcr:content/translations/en.DM00213525.pdf

STMicroelectronics. (2016b). *RM0090 reference manual: STM32F405/415, stm32f407/417, stm32f427/437 and stm32f429/439 advanced arm©-based 32-bit mcus*. Retrieved from http://www.st.com/content/ccc/resource/technical/document/reference_manual/3d/6d/5a/66/b4/99/40/d4/DM00031020.pdf/files/DM00031020.pdf/jcr:content/translations/en.DM00031020.pdf

STMicroelectronics. (2016c). *STM32F405xx/stm32f407xx*. Retrieved from http://www.st.com/content/ccc/resource/technical/document/datasheet/ef/92/76/6d/bb/c2/4f/f7/DM00037051.pdf/files/DM00037051.pdf/jcr:content/translations/en.DM00037051.pdf

STMicroelectronics. (2016d). *UM1472 user manual: Discovery kit with stm32f407vg mcu*. Retrieved from http://www.st.com/content/ccc/resource/technical/document/user_manual/70/fe/4a/3f/e7/e1/4f/7d/DM00039084.pdf/files/DM00039084.pdf/jcr:content/translations/en.DM00039084.pdf

STMicroelectronics. (2016e). *UM1725 user manual: Description of stm32f4xx hal drivers*. Retrieved from http://www.st.com/content/ccc/resource/technical/document/user_manual/2f/71/ba/b8/75/54/47/cf/DM00105879.pdf/files/DM00105879.pdf/jcr:content/translations/en.DM00105879.pdf

STMicroelectronics. (2016f). *UM1730 user manual: Getting started with stm32cubef4 firmware package for stm32f4 series.* Retrieved from http://www.st.com/content/ccc/resource/technical/document/user_manual/96/03/db/05/12/8d/40/9a/DM00107720.pdf/files/DM00107720.pdf/jcr:content/translations/en.DM00107720.pdf

Tomaszewski, D. (2007). Electrical characterization of ISFETs. *Journal of Telecommunications and Information Technology,* 55–60. Retrieved from http://dlibra.itl.waw.pl/dlibra-webapp/Content/287/JTIT-2007_3_55.pdf

Villalpando, J., Miranda, M., Martinez, M., & Martinez, H. (2012). ISFET sensor characterization. *Procedia Engineering, 35,* 270–275. doi: http://dx.doi.org/10.1016/j.proeng.2012.04.190

WINSENSE. (2016). *Ion sensitive field effect transistor (isfet): Winsense isfet pH sensor (wips).* Retrieved from http://tmec.nectec.or.th/public/uploaded/products/isfet/ISFET2016/ISFET\%20pH\%20Sensor.pdf

Yusof, K. A., Noh, N. I. M., Herman, S. H., Abdullah, A. Z., Zolkapli1, M., & Abdullah, W. F. H. (2013). pH Sensing and Characteristics of Silicon and Nitride Thin and Film and Silicon and Nitride-based ISFET and Sensor. In *2013 ieee 4th control and system graduate research colloquium, 19 - 20 aug. 2013, shah alam, malaysia.* IEEE. doi: 10.1109/ICSGRC.2013.6653290